Experimental Relations between Physical Structure and Mechanical Properties of a Huge Number of Drawn Poly(ethylene terephthalate) Yarns

H. M. HEUVEL,[1]* L. J. LUCAS,[1] C. J. M. VAN DEN HEUVEL,[1] and A. P. DE WEIJER[2]

[1]Akzo Research Laboratories Arnhem, Velperweg 76, Postbus 9300, 6800 SB Arnhem, The Netherlands, and
[2]Department of Analytical Chemistry, University of Nijmegen, Toernooiveld, 6525 ED Nijmegen, The Netherlands

SYNOPSIS

The results of a study of the relation between a number of mechanical properties of poly(ethylene terephthalate) (PET) yarns and their physical structure are presented. The relation was studied on a set of 295 drawn yarn samples, resulting from an exceptionally large variety in process conditions applied. The size of this experiment offered a unique opportunity to study the property–structure relation more extensively than ever before. Therefore, our understanding of the mechanical properties could be enriched with several new insights. A selection of seven yarn properties has been investigated. Five of them have been derived from the stress–strain curves and the remaining two are shrinkage and shrinkage force. The physical structure has been described with a set of five, statistically selected, parameters. Most of the yarn properties could very well be described in terms of these structure parameters. This description was performed by means of an artificial neural network, ANN. The type of calculation is completely naive, i.e., without any specific mathematical formulation for the relation concerned. The fitting results have been translated into physical aspects related to the well-known molecular two-phase model. The practical importance of a good physical understanding of yarn properties is that the essential possibilities and impossibilities of combinations of properties can far more easily be surveyed and understood. As a result, the efficiency of process developments can be substantially improved.

INTRODUCTION

In the past, various mechanical yarn properties such as modulus and shrinkage[1] have been described in terms of structural parameters related to the two-phase structure as depicted in Figure 1. Recently, a large experiment, comprising 295 drawn poly(ethylene terephthalate) (PET) yarns, was performed to cover a very wide range of structures and properties. This exceptionally large PET experiment, carried out under a variety of process conditions, offered a unique opportunity to study this relation much more intensively, leading to various essentially new insights. This paper presents, for a choice of mechanical properties, the relations with a set of carefully selected structural parameters. The set was obtained by using the results of a statistical component analysis (PCA), providing a minimum number of almost independent structural parameters capable of covering nearly all structural aspects.

To relate the mechanical properties to structure parameters, use has been made of an artificial neural network. This rather new type of computation technique, described in detail elsewhere,[2] works without any specific mathematical model. From the trained networks, it could easily be learned what variations in each of the mechanical properties can be achieved by varying each of the five structural parameters.

The numerical results have been interpreted in molecular terms within the well-known two-phase model for partially crystalline flexible polymers. Because of the general nature, this insight into the

* To whom correspondence should be addressed.

Journal of Applied Polymer Science, Vol. 45, 1649–1660 (1992)
 CCC 0021-8995/92/091649-12$04.00

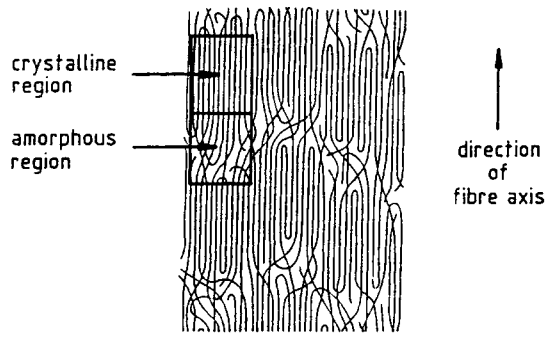

Figure 1 Schematic picture of the two-phase model of drawn PET yarns.

relations between physical structure and resultant mechanical responses may also contribute to a better understanding of the properties of yarns made from other semicrystalline polymers with flexible chains.

PHYSICAL YARN MODEL AND STRUCTURE PARAMETERS

For the description of the physical structure of the PET yarns, use is made of the two-phase model as depicted in Figure 1. In that model, well-ordered crystalline regions alternate with less ordered amorphous domains. Single molecules pass from several crystalline to amorphous regions, thus providing the coherence within the fiber. Depending on process conditions, the molecules are more or less oriented along the fiber axis. In this way, the so-called fibrils, i.e., structural units in which the coherence of amorphous and crystalline domains is found predominantly in a longitudinal direction, are formed. The crystalline regions can be regarded as homogeneous stiff blocks. The amorphous regions are quite different. Two aspects should be especially considered. The first is that the regions are inhomogeneous and, consequently, the orientation and tie chain length of the molecules have to be described by distributions instead of single numbers. It is clear that the inhomogeneity causes a distribution of stresses over the molecules in the amorphous regions on mechanical loading. This lack of molecular cooperation makes the amorphous regions the weak spots in fibers, consisting of flexible molecules, in a two-phase structure.

The second special aspect is that the molecules in the amorphous regions have some freedom to move. This permits, at increasing temperature, and especially above the glass transition temperature, the molecules to pursue configurations of enhanced probability, which means that on heating straight molecules will tend to coil.

From the foregoing it follows that for PET yarns the mechanical response on loading or heating is primarily determined by the amorphous phase. Therefore, for the description of mechanical properties, special attention is paid to the amorphous regions.

Many different structural parameters have been measured for all 295 samples of this series. Of course, between many of them, some correlations exist. For an effective characterization of the structure, a minimum number of independent structure parameters had to be found with which the structure can be described as completely as possible. To this end, the entire set of structure parameters has been subjected to a component analysis (PCA). On the basis of this analysis, the following set of parameters has been chosen:

1. The volume fraction of amorphous material.
2. The yarn viscosity as a measure of the length of the molecules.
3. The amorphous orientation factor.
4. The contour-length distribution factor of the tie chains between successive crystals.
5. The average volume of the individual amorphous regions.

As these structural aspects are very essential to understand the eventual results, each of them will be discussed separately and illustrated by very simple drawings of isolated fibrils in extreme situations.

Sub. 1. Volume Fraction of Amorphous Material ($1 - V_c$) (See Fig. 2)

This is the fraction of less ordered and more mobile material. In practice, this quantity varies only slightly in drawn yarns, viz. between 0.60 and 0.67 in this series.

Sub. 2. Yarn Viscosity, η_{rel} (See Fig. 3)

This quantity is a measure of the length of the molecules in the yarn. The parameter is important with respect to the number of chain ends in the amorphous regions and varies within this series between 1.55 and 1.86. Based on a relation between the degree of polymerization and the relative viscosity, it can be calculated that the viscosity values correspond to average molecular lengths of 1100 and 1800 Å, respectively. The relation mentioned was obtained by fitting polymerization degrees, as determined by end-group titrations and NMR measurements, to

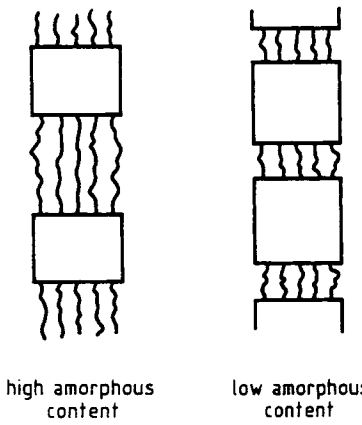

Figure 2 High and low amounts of amorphous material.

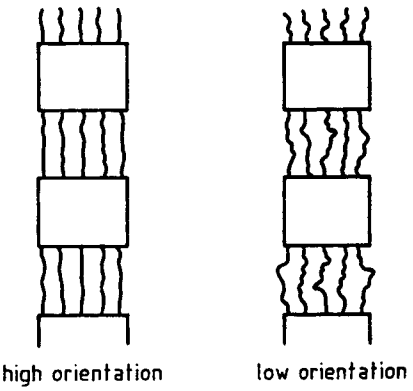

Figure 4 High level and low level of orientation of the tie molecules in the amorphous domains.

the corresponding relative viscosities.[3] Simple calculations indicate that at a yarn visco of 1.55 and of 1.86 at most 75% and 85%, respectively, of the (tie) molecules really connect successive crystals without being interrupted by chain ends. These numbers hold for average dimensions of crystals and amorphous domains and are even lower for coarser structures.

Sub. 3. Amorphous Orientation Factor, Fas (See Fig. 4)

In the amorphous regions, the molecular segments can be oriented at a great variety of angles with respect to the fiber axis. Therefore, there is a distribution of direction angles and, experimentally, only numbers can be obtained that are related to certain averages of the cosines of these angles over the entire distribution such as $\langle \cos^2 \varphi \rangle$ or $\langle \cos^4 \varphi \rangle$, where φ is the angle between the molecular segment and the fiber axis as shown in Figure 5.

Therefore, for a perfectly aligned segment $\varphi = 0$, $\cos \varphi = 1$, and for less oriented segments, the cosine values are lower. Consequently, the less oriented segments contribute less to a $\langle \cos^4 \varphi \rangle$ than to a $\langle \cos^2 \varphi \rangle$; e.g., at $\varphi = 30°$, $\cos^4 \varphi = 0.56$ and $\cos^2 \varphi = 0.75$. The overall result is that in a $\langle \cos^4 \varphi \rangle$ the emphasis is much more on the best-oriented molecules than in a $\langle \cos^2 \varphi \rangle$. This fact is of practical importance as we used two different techniques for the orientation measurements, viz. birefringence and sonic modulus. Birefringence, leading to the orientation factor Fab, is only a function of $\langle \cos^2 \varphi \rangle$, whereas in the sonic modulus, leading to the orientation factor Fas, a combination of $\langle \cos^2 \varphi \rangle$ and $\langle \cos^4 \varphi \rangle$ is involved.[4] As a measure of the level of the amorphous orientation, the factor based on sonic measurements, Fas, has been chosen rather arbitrarily. This value can theoretically vary from zero for fully unoriented to one for perfectly oriented situations. In practice, this orientation parameter varied from 0.69 to 0.83 in this series of drawn yarns.

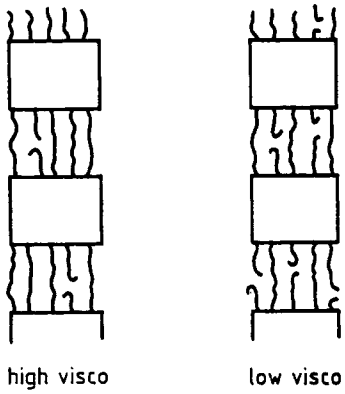

Figure 3 High and low yarn visco, resulting in many or only a few uninterrupted tie molecules.

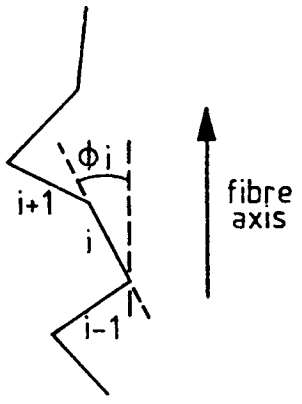

Figure 5 φ_i is the angle between segment i of a tie molecule and the direction of the fiber axis.

Sub. 4. Contour Length Distribution Factor, Fas/Fab (See Fig. 6)

As no technique exists for the direct measurement of the tie chain-length distribution, we tried to evaluate some related quantity.

As discussed in an earlier paper,[1] we found by infrared spectroscopy and by the combination of sonic modulus and birefringence measurements that the orientation distribution in drawn yarns, spun at higher winding speeds, is broader. Therefore, the ratio of Fas/Fab, reflecting the combination of sonic modulus and birefringence, was studied in relation to winding speed, and this quantity was found to increase systematically with that process condition. Consequently, this ratio was considered to be related to the width of the orientation distribution in the amorphous phase. Of course, this quantity cannot be proved to represent directly all aspects of the orientation distribution, but we consider it as a quantity roughly representing the aspect of the width of the orientation distribution in a first approximation. As can be seen from Figure 6, this orientation distribution should be related, at least in a qualitative way, to the contour-length distribution. The figure illustrates that a broad tie chain-length distribution, comprising straight taut molecules together with long loose loops, requires spatially also an appreciably broader orientation distribution. Therefore, we eventually chose the Fas/Fab ratio as a practical, easy to measure, factor representing somehow the aspect of the width of the contour-length distribution of the tie chain molecules. In this series, the indicator Fas/Fab varies from 1.12 for narrow distributions to 1.68 for the broadest.

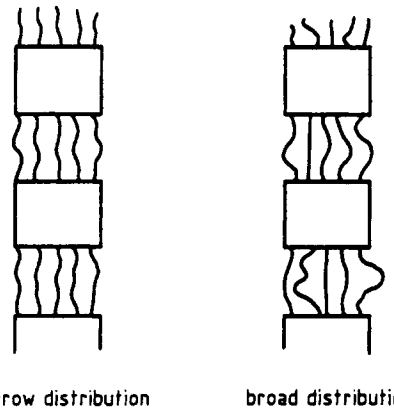

Figure 6 Different orientation distributions that are related to different contour-length distributions of the tie chains.

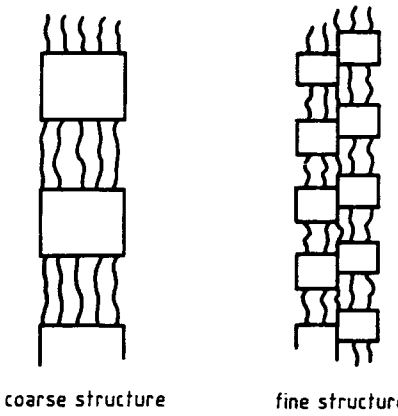

Figure 7 The coarseness of the structure is determined by the sizes of both the individual crystalline and the individual amorphous regions.

Sub. 5. Size of the Individual Amorphous Regions, G (See Fig. 7)

The structure of a yarn can vary from fine to coarse, depending on the sizes of the individual amorphous and crystalline domains. Experimentally, the average size of the crystals in a yarn can easily be determined by X-ray diffraction. This size is proportional to the product of the average lengths of the crystals in its three main directions. Assuming there is no amorphous matrix, the two-phase model implies that the volume of the individual amorphous regions equals that of the crystals, multiplied by the ratio of the total amount of amorphous and crystalline material. Therefore, the average volume of the individual regions is proportional to

$$\Lambda_{100} \times \Lambda_{010} \times \Lambda_{\bar{1}05} \times \frac{1 - V_c}{V_c}$$

where the Λ's indicate the crystal dimensions, and V_c, the crystallinity. This quantity varies in this series between 4.6 and 14.4 $\text{Å}^3/10^5$.

General Remarks

The aforementioned parameters, chosen for the description of mechanical properties, are related to the amorphous phase. This does not imply that the crystals are not important. The crystallinity and the size of the crystals directly determine the amount of amorphous material and the coarseness of the structure, respectively.

EXPERIMENTAL

Production of the Yarns

The 295 drawn PET yarns have been produced by applying a large variety in process conditions; especially, chip viscosity, winding speed, draw ratio, drawing temperature, and degree of relaxation have been varied.

Yarn Properties

As mechanical properties to be described in terms of structural parameters, the following quantities have been taken into consideration:

Mod-1: first maximum of the modulus–strain curve (mN/tex).

Mod-2: second maximum of the modulus–strain curve (mN/tex).

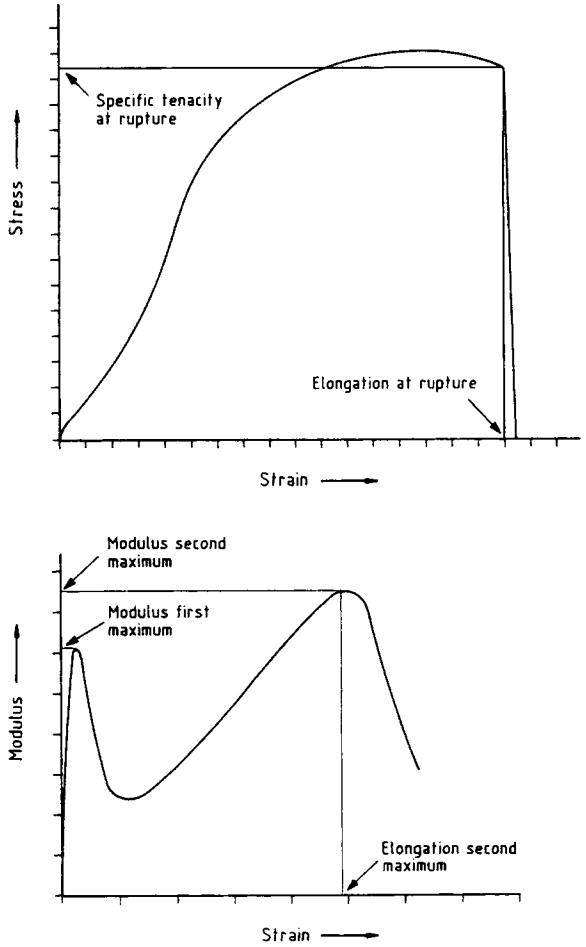

Figure 8 (a) Stress–strain and (b) modulus–strain curve.

El-Mod-2: elongation at the second maximum of the modulus–strain curve (%).

Ten-ru: specific tenacity at rupture (mN/tex).

El-ru: elongation at rupture (%).

HAS-160: hot-air shrinkage at 160°C (%).

HAST-160: shrinkage force at 160°C (mN/tex).

The mechanical yarn properties were measured on conditioned yarns (16 h at 21°C and 60% RH) using an Instron tensile tester. The yarn pretension was 5 mN/tex; the gauge length, 500 mm, and the crosshead speed, 500 mm/min. The measurements were performed on yarns with a twist level of Z60. The stress–strain measurements resulted in two curves for each sample: a stress–strain curve and its first derivative, i.e., the modulus–strain curve, as depicted in Figure 8(a) and (b), respectively. In this figure, the various mechanical properties are indicated.

The thermomechanical properties have been determined at 160°C on a Zwick contractiometer with a length of 400 mm clamped at a load of 5 mN/tex. For the shrinkage HAS-160, the length of the loaded sample was measured after 4 min, while the yarn was still in the furnace. For the shrinkage force, HAST-160, the yarn was kept at constant length and the maximum force occurring after 4 min was recorded.

Structure Parameters

As discussed before, the following structure parameters have been used for the description of the yarn properties:

1. Volume fraction of amorphous material.
2. Yarn viscosity as a measure of the length of the molecules.
3. Amorphous orientation factor.
4. Contour-length distribution factor of the tie chains between successive crystals.
5. Average volume of the individual amorphous regions.

Sub. 1. The volume fraction of amorphous material was determined as

$$1 - V_c = 1 - \frac{d - d_a}{d_c - d_a} \qquad (1)$$

The overall density d of the yarns was determined in a density gradient column, containing a mixture

of tetrachloromethane/*n*-heptane at 23.0°C. The crystalline density, d_c, was obtained from WAXS, combined with curve-fitting, as discussed in Ref. 1.

Sub. 2. Relative viscosities were determined as solutions of 1 g PET in 100 g *m*-cresol at 25.0°C.

Sub. 3. According to Dumbleton,[5] and taking into account that the amorphous density is slightly orientation-dependent, the following formula can be derived:

$$\text{Fas} = \frac{d_c - d + 0.495(1 - f_c)(d - 1336) - \dfrac{2.73}{E}(d_c - 1336)}{d_c - d + 0.495(1 - f_c) \times 9.4 - \dfrac{2.73}{E} \times 9.4} \quad (2)$$

The sonic modulus E is determined as $E = dV^2$, where V is the propagation velocity of a pulse wavefront (10 kHz) traveling through the yarn. The crystalline orientation factor f_c was constant within this experiment at the value of 0.985.

Sub. 4. As a measure of the tie chain-length distribution, the quantity Fas/Fab was used. The expression for Fas has already been given as formula (2). For the birefringence amorphous orientation factor Fab, the formula

$$\text{Fab} = \frac{\Delta n - 0.22 f_c V_c}{0.275(1 - V_c)}$$

is used,[3] according to Stein and Norrism,[6] where Δ_n is the birefringence obtained with a de Senarmont compensator; f_c, the crystalline orientation factor, being constant at a value of 0.985; and V_c, the crystallinity as described at Sub. 1. The constants used are those determined by Dumbleton.[5]

Sub. 5. The average volume of the individual amorphous regions is calculated as $(1 - V_c)/V_c \cdot \Lambda_{100}$ Λ_{010} $\Lambda_{\bar{1}05}$, where Λ_{100} and Λ_{010} are crystal thicknesses, and $\Lambda_{\bar{1}05}$, the crystal height of the PET crystals.

RELATIONS BETWEEN MECHANICAL PROPERTIES AND PHYSICAL STRUCTURE

One of the major objectives of this work was to investigate the separate effects of the various structural aspects on a variety of mechanical properties and to understand the results physically. As discussed before, five parameters have been selected to describe the total physical structure. To get a first impression of the influence of these parameters on the mechanical properties, every mechanical property has been plotted vs. the five structural parameters. As an example, in Figure 9, the plots for the tenacity at rupture are shown. It can be seen that the information extractable from these plots is very limited. To improve the output, use has been made of an artificial neural network (ANN). Since 1986, ANNs have been used mainly for classification purposes. A new development is the application[2] as a soft modeling technique for predicting purposes, as in this case, mechanical properties from structural data. ANNs differ from other approaches by learning from examples.[7] The computer simply runs through the examples again and again and learns from the mistakes it made in past trials by adapting the various weights of the interneural connections. Therefore, they are naive, initially model-deficient systems, not restricted by prior conditions. No time or effort has to be spent on developing mathematical formulations of unknown relations as necessary in, e.g., nonlinear regression. More details can be found in the special paper cited before.[2]

The differences between the experimental values of the yarn properties and those calculated by the trained ANN are almost completely due to experimental errors in the measurements of mechanical properties and structure parameters. Therefore, in other words, the lack of fit of the trained ANN is almost negligible.

To obtain a realistic impression of the influence of each of the structure parameters, the trained ANN has been applied. One of the five structure parameters is, as input, varied over the total experimental range, while the other four parameters are kept constant at their average values. The trained ANN shows in that case the course of the property involved as a function of the structure parameter varied. Therefore, the separate effects of the five structure parameters can be obtained for each of the mechanical properties. Of course, between the structure parameters selected, some correlation also exists and, consequently, the technique of varying one parameter and keeping the others constant is not perfectly realistic. Yet, the results can be regarded as reliable indicators because the application of PCA favored the independence of the structure parameters as much as possible. This was also indicated by the results of a factorial design, applied in combination with the trained network.[2] It showed that the pure effects mostly appreciably surpass those described by combinations of structure parameters.

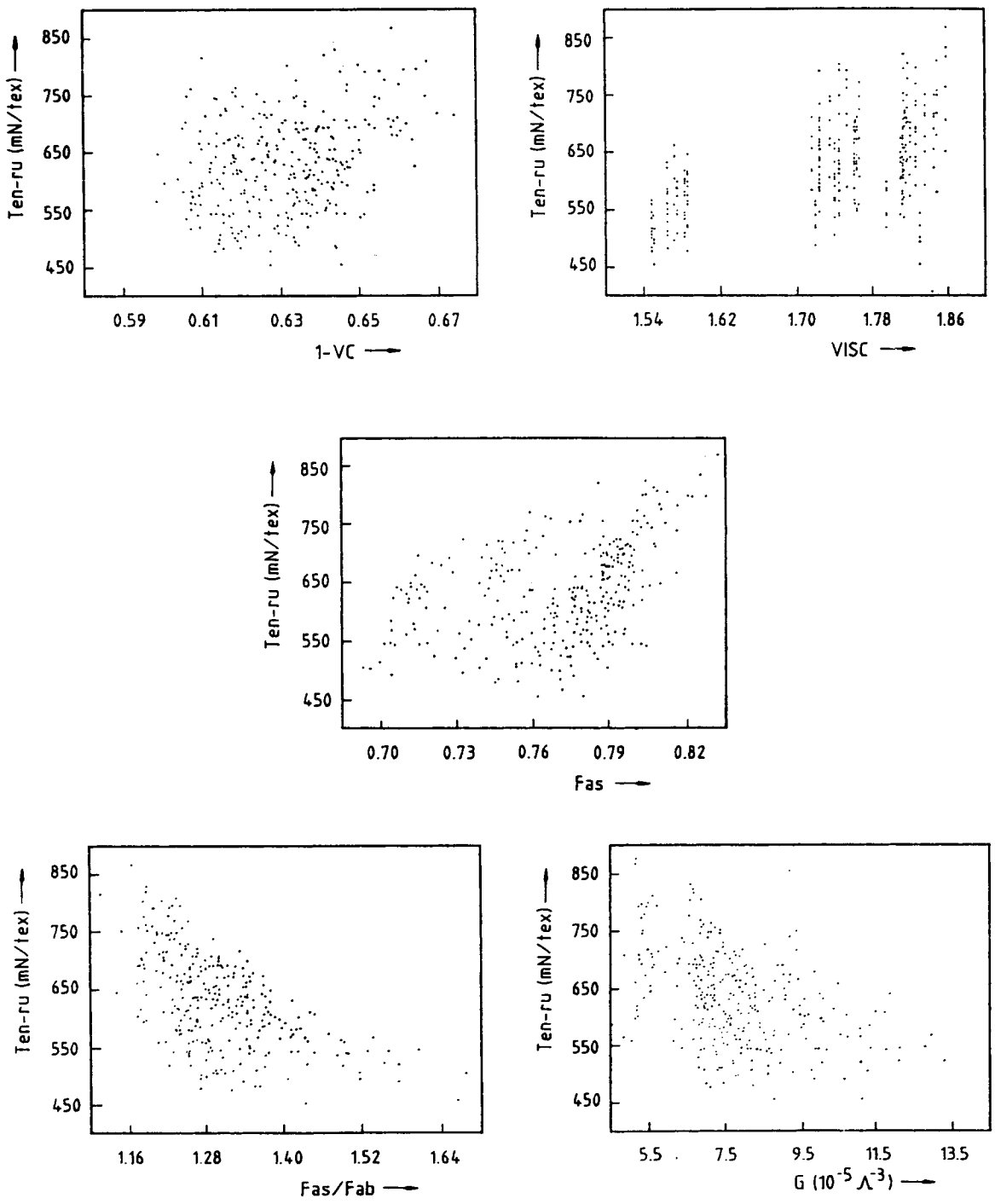

Figure 9 Tenacity at rupture plotted vs. the five structural parameters.

RESULTS

As described above, the overall effect of each structure parameter can be shown by the trained ANN, by varying one structure parameter over the experimental range while the other four structure parameters are kept constant at average values. Such a result is shown in Figure 10, where the tenacity has been plotted vs. each of the structure parameters, varied over the entire experimental range. Similar

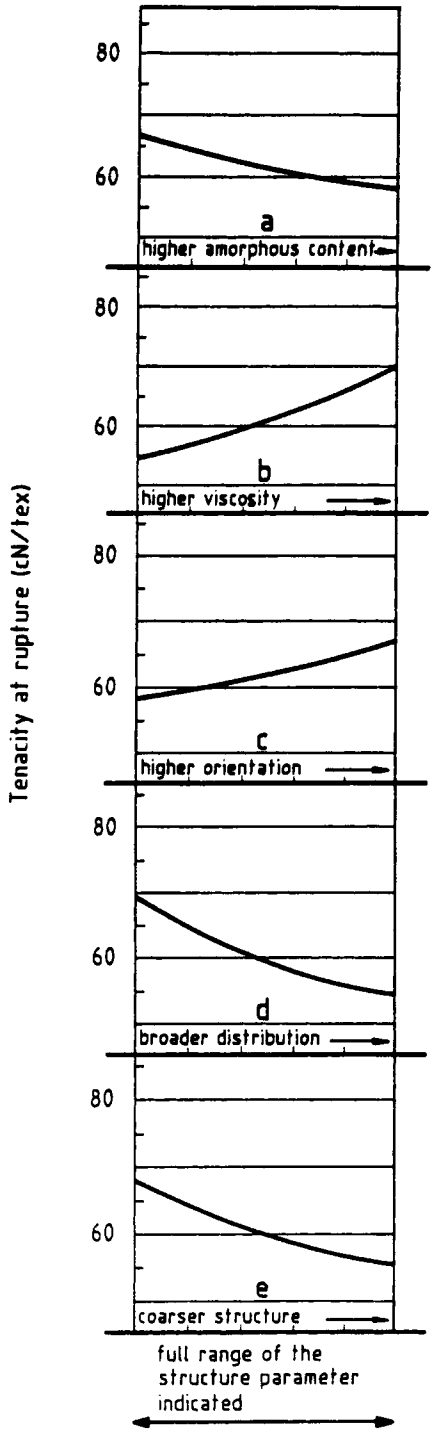

Figure 10 The influence of the five structure parameters on the tenacity at rupture.

pictures can be made for all other mechanical properties. However, for an easy survey, another way of presentation has been chosen. The difference of the property values, measured at maximum and at minimum values of the structure parameter, is presented in a bar diagram as a percentage of the total experimental property range. In Figure 11, the results for all mechanical properties are presented. If the bar indicates a negative contribution, this means that an increase of the structure parameter causes a decrease of the property.

QUALITATIVE INTERPRETATION OF THE RESULTS IN TERMS OF THE TWO-PHASE MODEL

Earlier, various mechanical properties such as modulus, shrinkage, and tenacity were studied as functions of structural parameters. Most of those investigations were limited to sets of experiments that were much smaller than the set discussed in this paper. Therefore, in the earlier investigations, for some properties, a physical structure picture was obtained that turned out to be very useful in practice.[1] This large experiment, however, offered the opportunity to study a larger number of mechanical properties and each of them in more detail than was possible before. In the following, the major effects as presented in Figure 11 are interpreted in terms of the two-phase model described before.

Stress–Strain Properties

The first five mechanical properties of the set mentioned before are related to the stress–strain behavior of the yarns. In Figure 8(b), the first derivative of the stress–strain curve, i.e., the modulus–strain curve, is given. Clearly, two maxima are seen that can be attributed to two different mechanisms. According to unpublished work,[8] the first maximum can be related to straining of an entanglement network in the sense of Ball et al.[9] (see Fig. 12). After breaking up of the entanglements, the tie molecules proper, connecting successive crystals, are strained, the mechanism of which shows up in the second peak of the modulus–strain curve. Using this picture, and reasoning in terms of the two-phase model, the results presented in Figure 11 will be discussed. In this way, the understanding, on a molecular scale, of various mechanical properties can be substantially improved.

First Maximum of the Modulus–Strain Curve (Mod-1)

Already at a very low strain of about 0.6%, the first maximum in the modulus–strain curve is found. This

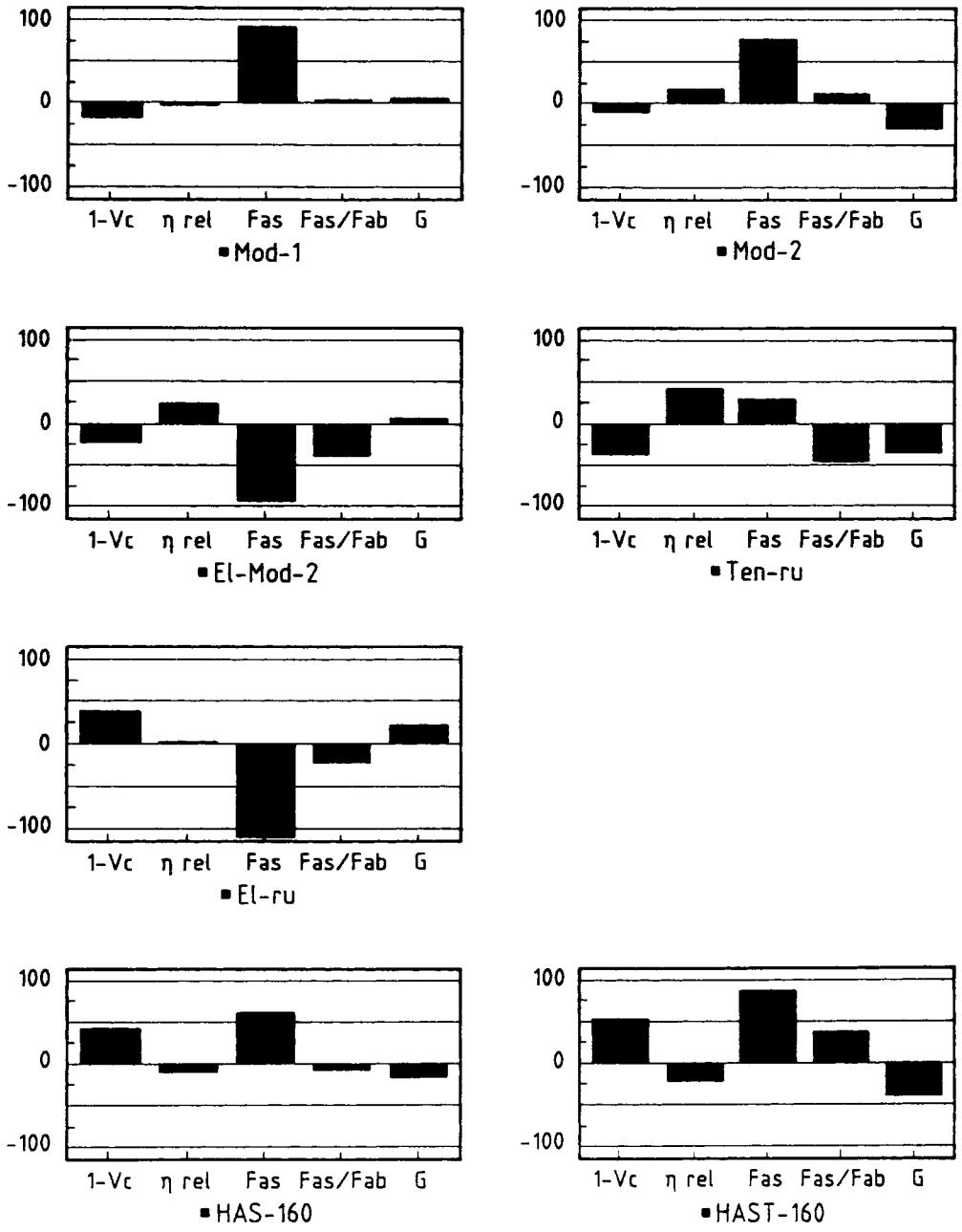

Figure 11 Overview of the maximum attainable effects of the five structure parameters on all mechanical yarn properties in percentages of the experimental ranges.

strain level hardly varies within the set of yarns. Therefore, it is concluded that disintegration of the entanglement network starts at a strain that is independent of the structure parameters varied. From Figure 11 it follows that for the modulus value of the first maximum the orientation of the molecules is very important. Our tentative interpretation of this orientation effect is that orientation promotes the formation of a denser network. Breaking down a denser network requires a higher force as it contains more physical cross-links. This higher force causes a higher modulus because the elongation at the first maximum is constant. Figure 11 also reveals a positive effect for a low value of $(1 - V_c)$, i.e., for a high crystallinity. This can be understood from the fact that crystals can be regarded as stiff blocks, having a much higher modulus than that of the amorphous domains.

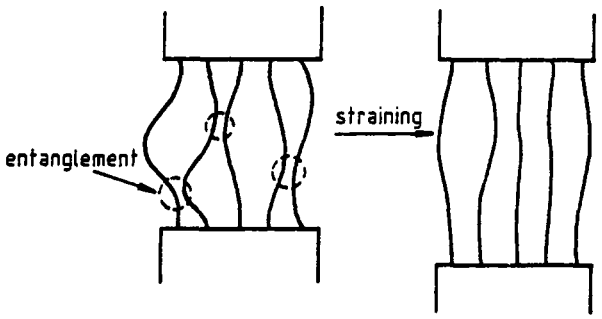

Figure 12 Breaking up of the entanglement network.

Second Maximum of the Modulus–Strain Curve (Mod-2)

In the second part of the modulus–strain curve, the tie molecules are directly addressed. The strain at which the maximum occurs can vary considerably, ranging in this series from 3 to 14%. For a maximum, positioned at a high strain level, the force is built up very gradually and the increase of force per unit of increase of strain, being the modulus, is low. This is illustrated in Figure 13. Therefore, a low orientation, which is the main reason for a high strain level, causes a low Mod-2 value. In the same way, a positive contribution is obtained from a broad contour-length distribution factor, giving rise to a low value of the elongation at the second maximum in the modulus–strain curve. The positive effect of the visco can be translated into a larger number of tie molecules, offering more resistance to straining. Another significant contribution is found in the coarseness of the structure. Based on dynamic FTIR measurements[10] and the results of SEC investigations,[11] it is supposed that the second maximum is due to the first fracture of the tie molecules. In that picture, this effect can be understood from the fact that small amorphous regions keep the effect of molecular fracture limited to a small sphere of action, as depicted in Figure 14. The positive effect of a higher crystallinity can be understood in the same way as already discussed for the Mod-1 property.

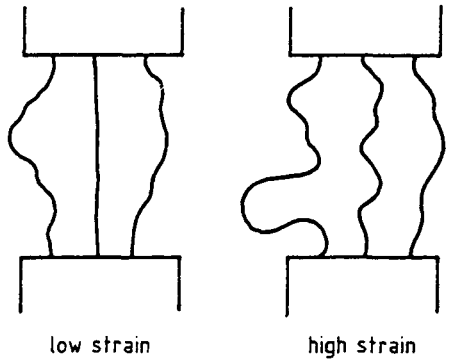

Figure 13 Straining the less oriented situations leads to a more gradual buildup of the straining force and, consequently, to a lower modulus.

Elongation at the Second Maximum of the Modulus–Strain Curve (El-Mod-2)

Of the elongation at which the second peak in the modulus–strain curve is found, only the two major contributions are well understood. As described earlier for Mod-2, we assume that the maximum is related to fracture of the shortest tie molecules. The combination of a low level of orientation and a narrow distribution provides the situation where the shortest tie molecules have relatively the greatest contour length, as illustrated by the asterisk in Figure 15. Therefore, the first fracture of tie molecules can be expected to occur at relatively high strain values for structures with low orientations combined with narrow tie chain-length distributions.

So far, the influence of the structure has been conceivable. The smaller effects of visco and crystallinity are not yet well understood.

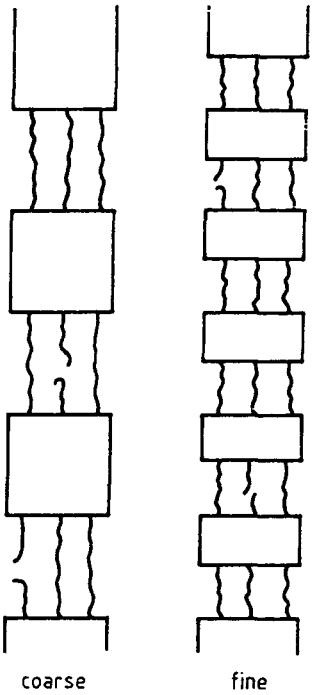

Figure 14 Crystal boundaries determine the action domains of broken molecules.

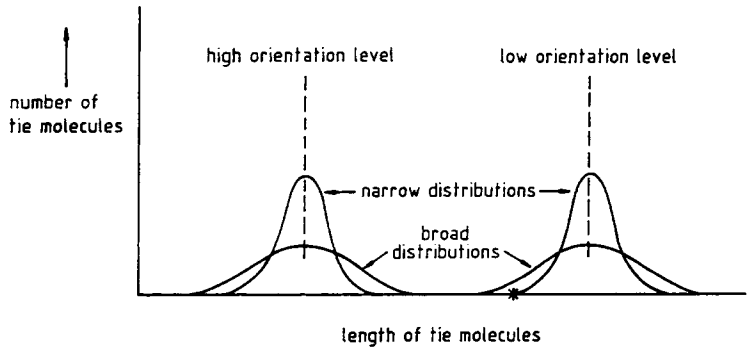

Figure 15 Combination of low orientation level and narrow distribution gives the greatest possible contour length (*) for the shortest tie molecules of the various distributions.

Specific Tenacity at Rupture (Ten-ru)

Rupture is supposed to be initiated by amorphous regions in which the tie molecules have been broken. To achieve this, a higher force is needed

- if more tie molecules are present, i.e., at a higher viscosity,
- if they carry the load together instead of one after the other, i.e., with a narrow tie chain-length distribution, and,
- if the effect of molecular fracture is confined to small action domains, i.e., not a coarse but a fine structure is favorable for high strength.

The effect of orientation is predominantly not direct, but related to its influence on the elongation at break. This connection is because tenacity has been defined as stress per unit of the cross-sectional area before elongating. As the high elongation at break causes a considerable decrease of the filament cross section at the moment of rupture, a low specific tenacity is found. The positive effect of the crystallinity may be because it contributes to a lower elongation at break and because less material is available in the amorphous phase where molecular rupture can only take place.

Elongation at Rupture (El-ru)

A yarn with a large fraction of deformable material that is poorly oriented will have a large elongation at rupture. This is what Figure 11 shows as a positive contribution of $(1 - V_c)$ and a negative one of Fas. The effects of contour-length distribution and coarseness of the structure are not well understood at the moment.

Shrinkage Properties

In this section, the shrinkage behavior of the PET yarns is described in terms of structural parameters. At the temperatures considered, the polymer is far above the glass transition temperature. Under such circumstances, the behavior of the yarn is dominated by the tendency of straight parts of molecules present in the mobile, i.e., amorphous, phase to coil in order to gain entropy. If a yarn is free to change its length, this coiling leads to shrinkage, but if the length is fixed, it causes a shrinkage force.

Hot-air Shrinkage at 160°C (HAS-160)

Shrinkage increases with orientation of the molecules within the amorphous regions because the effect of coiling is most pronounced when starting with more straight parts of tie molecules. If more molecules are in the mobile phase, i.e., when $(1 - V_c)$ is larger, the effect of coiling is stronger and a higher shrinkage can be expected. Also, a narrow tie chain-length distribution is indicated in Figure 11 as slightly favorable for a high shrinkage. This suggests that coiling takes place as a collective process, which is not surprising because the density difference between the amorphous and crystalline phase amounts to not more than 10%. As a result, there is hardly any room available for an individual molecule to coil effectively. The need of collective movement can best be met by molecules having about the same length; therefore, by a narrow tie chain-length distribution. The contribution by a low G value may be because at 160°C the smallest crystals already start to melt, providing oriented material with a high tendency to coiling. With respect to the influence of the viscosity, it may be relevant that at 160°C the molecular mobility is still rather low. At this low level, some sig-

nificant increase of mobility is possibly realized by more chain ends, i.e., by a lower viscosity.

Shrinkage Force at 160°C (HAST-160)

For the shrinkage force, only the tendency toward coiling is important. This means that the collective action is not relevant here and a narrow distribution of chain lengths is no longer needed. On the contrary, a broad distribution will, at a given level of orientation, provide relatively short, straight molecules that highly contribute to the shrinkage force. The effect of the coarseness of the structure is not well understood here.

The authors gratefully acknowledge all co-workers of the laboratories who carried out the many measurements that formed the basis for this study, F. A. T. Lijten, A. Roos, and M. H. J. van den Tweel for their initiative to and realization of this large set of yarns, R. Huisman and J. A. Juijn for the discussions that contributed substantially to the eventual results, and A. Bezemer, J. M. Woestenenk, and G. Ruitenberg who supported and strongly encouraged this type of work from the very beginning.

REFERENCES

1. R. Huisman and H. M. Heuvel, *J. Appl. Polym. Sci.*, **37,** 595 (1989).
2. A. P. de Weijer, L. Buydens, G. Kateman, and H. M. Heuvel, *Chemolab,* to appear.
3. C. Duvekot and K. C. J. B. Lind, Internal Akzo report, March 1970.
4. I. M. Ward, *Mechanical Properties of Solid Polymers,* Wiley-Interscience, London, 1971, p. 254.
5. J. H. Dumbleton, *J. Polym. Sci. A-2,* **6,** 795 (1968).
6. R. S. Stein and F. H. Norrism, *J. Polym. Sci.*, **21,** 381 (1956).
7. D. E. Rumelhart and J. L. McClelland, *Parallel Distributed Processing Exploration in the Microstructure of Cognition,* Cambridge, MA, MIT Press, 1986, Vol. I.
8. L. J. Lucas and J. G. M. van Miltenburg, unpublished results.
9. R. C. Ball, M. Doi, S. F. Edwards, and M. Warner, *Polymer,* **22,** 1010 (1981).
10. W. A. Faassen and C. J. M. van den Heuvel, unpublished results.
11. C. J. M. van den Heuvel, unpublished results.

Received May 6, 1991
Accepted October 10, 1991